FINAL REPORT

ELECTRODEPOSITION IN MICROGRAVITY
(Ground-Based Experiments)

NATIONAL AERONAUTICS AND SPACE ADMINISTRATION

CONTRACT NUMBER NAS8-33812

May 13, 1981 - June 30, 1982

by

Clyde Riley
Professor of Physical Chemistry

and

H. Dwain Coble
Associate Professor of Inorganic Chemistry

University of Alabama in Huntsville

Huntsville, Alabama 35899

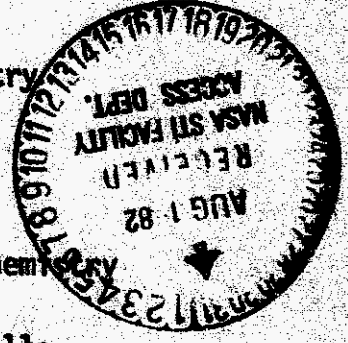

June, 1982

DRAFT

FINAL REPORT

ELECTRODEPOSITION IN MICROGRAVITY
(Ground-Based Experiments)

NATIONAL AERONAUTICS AND SPACE ADMINISTRATION

CONTRACT NUMBER NAS8-33812

May 13, 1981 - June 30, 1982

by

Clyde Riley
Professor of Physical Chemistry

and

H. Dwain Coble
Associate Professor of Inorganic Chemistry

University of Alabama in Huntsville

Huntsville, Alabama 35899

June, 1982

NASA Contract
NAS8-33812
Final Report

ABSTRACT

Electrodeposition has been studied at 10^{-2} g and compared with bench studies at 1 g. The low gravity was achieved during KC-135 aircraft parobolic flights. Flow in a simple cobalt cell (1 M $CoSO_4$) operating under typical commercial conditions (10-20 mA/cm^2 and < 1 V) was monitored with a Schlieren optical system. It vividly demonstrated that natural convection was absent at 10^{-2} g. Quantitative comparisons on a cobalt cell with shielded electrodes using interferometry were carried out. Fringe shift differences indicate greater semi-infinite linear diffusion at 1 g than at 10^{-2} g for cobalt. Since a shielded electrode operates under diffusion controlled conditions, no differences between 1 g and 10^{-2} g would be expected. Similar comparisons on a shielded electrode copper cell were inconclusive. We have begun bench codeposition experiments using polystyrene neutral buoyancy particles coupled with a shielded electrode cobalt cell. Tracking of 12 μm particles showed no measurable difference between thermal/Brownian motion when the cell was operational or nonoperational. Initial experiments on codeposition quality showed a strong dependence upon cathode surface preparation in a shielded electrode configuration.

TABLE OF CONTENTS

LIST OF FIGURES

Section 1
INTRODUCTION

1.1 Origin and Importance of Study

Gravity has a significant influence on electrochemical processes and in particular electrodeposition. During electrodeposition density gradients are created which result in convective transport that effects forming and surface preparations. Due to the magnitude of commerical activity involving electrodeposition preparations it is a logical candidate for studying the effects of reduced gravity and the possibility of capitalizing on any benefits.

With this consideration, Dr. Gordan Fisher of INCO Research and Development Center (Suffern, N.Y. 10901) initiated contact with the Space Sciences Laboratory of George C. Marshall Space Flight Center. Discussions with the Commerical Applications Office of the MPS Program resulted in a technical exchange agreement involving low g effects upon electrodeposition processes. This agreement subsequently evolved into a unique cooperative effort not only involving INCO and NASA but included the University of Alabama in Huntsville (UAH). The cooperation would involve private enterprise in a potentially benefical space processing project while utilizing the present facilities and expertise of all three groups in order to minimize effort and cost. The overall plan was for NASA and UAH to work out details of the experiments in consultation with INCO. Later, when hard results became available (e.g. low g or modeled low g electroplated surfaces) INCO would then participate more actively using their facilities for analysis and testing.

1.2 Scope of Work

The research conducted under this program is concerned with the investigation of electrodeposition (solution to solid and solution plus suspension to solid) in relation to electrodeposition in microgravity. The primary objectives of these studies were to obtain information concerning electrodeposits enabling evaluation of microgravity effects on the growth of electrodeposits in space. In particular we proposed to look at fluid flow (solution) as material left the solution phase and entered the solid. Likewise we desired to determine the quality of the electrodeposits.

Section 2
GENERAL

2.1 Electrodeposition and Gravity

Gravity influences electrodeposition only by convection for a simple metal-in, metal-out system. Convectionless electrodeposition cells can be created by utilizing shielded electrodes.[1] These systems have attracted attention because they enable one to study reactions under purely diffusive conditions,[2-6] which

in principle should be identical to those experienced in space. The method of choice for monitoring fluid flow is interferometry because it enables one to quantitatively evaluate concentration changes as a function of time. Schlieren methods may also be used to monitor concentration changes.[7-8] The latter have only qualitative value but offer the observer an immediate image conducive to physical interpretation as opposed to the fringe patterns of interferometry.

Gravity influences codeposition in two ways, convectively and through sedimentation. Due to potential improvements in coatings with metals containing neutrals, private industry has shown interest in the production and properties of electrocodeposits.[9-12] The behavior of these systems in microgravity can be benched-studied using shielded electrodes to obviate convection and neutral buoyancy particles to minimize sedimentation. Variables affecting the production of the codeposits in microgravity can be determined with this model, but obviously properties such as wear, or corrosion resistence of real systems, e.g. Co + Cr_3C_2, could not be determined unless a codeposit produced in microgravity over a period of several hours were available.

2.2 Simple Electrodeposition

In these studies the actual electrodeposition involves only simple metal-in, metal-out systems. Gaseous evolution and side reactions were non existent leading to:

$$M^{n+}(Aq) + ne^- \rightarrow M(s) \qquad \text{reduction} \qquad (1)$$

and

$$M(s) \rightarrow M^{n+}(Aq) + ne^- \qquad \text{oxidation} \qquad (2)$$

at the anode and cathode respectively. The variables that effect the quality of the deposits under these conditions are concentration, current density, pH and temperature. Holding the latter three variables constant, concentration becomes the variable of interest. Utilizing a shielded electrode to eliminate convection the instantaneous current i_t through a cell is given by:[1]

$$i = \frac{nFADo^{\frac{1}{2}}Co}{\pi^{\frac{1}{2}} t^{\frac{1}{2}}} \qquad (3)$$

where n is the electron change in reactions (1) and (2), F is Faraday's constant, A is electrode area, Do is the diffusion constant for M^{n+}, Co is the bulk concentration of M^{n+}, and t is the time in seconds. Hence one immediately

notices the influence of Co since $it^{\frac{1}{2}}$ is a constant for a given cell configuration and electrode system. This equation predicts the same results for a shielded electrode cell and a cell operating in microgravity. Differences could only result if Do is a function of gravity or if an unknown flow occurs in microgravity.

2.3 Codeposition

In these studies a neutral material (5-12 μm) is added to the simple oxidation/reduction system represented by equations (1) and (2). The only type of charge these particles could carry are zeta potentials, δ, which are associated with an immobile layer of ions that can stick tightly to the surface of any large neutral particle.[13] Snaith and Groves have proposed that inert particles are carried to the vicinity of the electrode solution interface (double layer) hydrodynamically in a stirred system (forced convection) and then transported through the double layer electrophorectically. The electrophoretic velocity is given by:

$$u = \frac{DE\delta}{4\pi\eta} \qquad (4)$$

where D is the dielectric constant of the medium, E is the potential gradient, δ is the zeta potential and η is the coefficient of viscosity for the liquid. In a diffusion controlled system the particle movement would be Brownian and this electrophoretic velocity through the double layer would dominate. For a well polished surface (free of undulations relative to particle size) one should expect a random adherence of these particles to the surface for subsequent entrapment in the matrix of the depositing metal M.

Guglielmi has formulated a qualitative model for codeposition.[14] Data displayed as volume % of inert in deposit versus volume % of the inert in the suspension demonstrate a nonlinear dependence upon concentration of the inert. The model explains the dependence of particle codeposition on solution composition in terms of the structure of the layer of molecules and ions absorbed on their surface on the electrode and indirectly on the composition of the solution. It assumes a moving medium and natural or forced convection does not effect the absorbed particles, and particle inclusion is not related to particle size.

2.4 Materials and Systems

The selection of systems to study was governed by the requirements of simplicity, commercial interest and scientific interest. Initial work was done

on the silver system with a subsequent shift to copper because of the literature data available for comparison. The cobalt system was chosen because of the interest to INCO.

3.1 Non Shielded Electrode Cells

Four cell variations have been designed or pieced from commerically available products during the contract period. Two more variations are still under construction. The first cell was a commerical fluorometric cell polished on four sides measuring 45 mm x 40 mm x 12 mm. Nickle wire leads with 1 cm^2 electrodes spaced 1 cm apart were glued through the sealing teflon cover. Typically, the electrodes consisted of a Cu anode plated with Co and a Cu cathode. All surfaces exposed to the electrolyte except the electrode faces were coated with nail polish (Figure 1). The cell was driven by a circuit which included a 1.5 V hobby battery, variable resistance box and a milliampmeter These cells were utilized to establish the utility of the Schlieren technique to detect mass flow.

3.2 Shielded Electrode Cells

Our first shielded electrode cell consisted of a hollow teflon tube 2 inches long and 1.256 inches I.D. Copper, cobalt or stainless steel electrodes were machined with cylindrical backs and flat faces with dimensions 1 cm wide and 2 cm long. The electrodes were mounted parallel and flush to the I.D. of the cylinder with brass threaded feed throughs screwed to the electrode backs. Distance between faces was exactly 1 cm. Two optical flats were used to enclose the electrodes with circular externally threaded screw plugs used to hold the plates firmly against the electrodes. Holes were drilled centrally and commerical IR cell fill ports were inserted to enable syringe filling. Figure 2 shows the cell. Holders consisting of ring clamps were cut to hold the cell in any position parallel to the cell axis. The same circuit to power the unshielded cell was utilized with a recorder added to monitor the current continuously. Figure 3 demonstrates schematically the difference between shielded and unshielded electrode cells in a horizontal configuration.

3.3 Neutral Buoyancy Shielded Electrode Cells

Several variations of this cell have been constructed ranging from complex to extremely simple. The most complex is still under construction by the glass maker. It involves precision cutting and grinding that will result in an all glass cell with four sided electrode cavity viewing. The simplist and perhaps

FIGURE 1

Early cell with unshielded electrodes.

FIGURE 2

Second cell. First variation of shielded electrode cell.

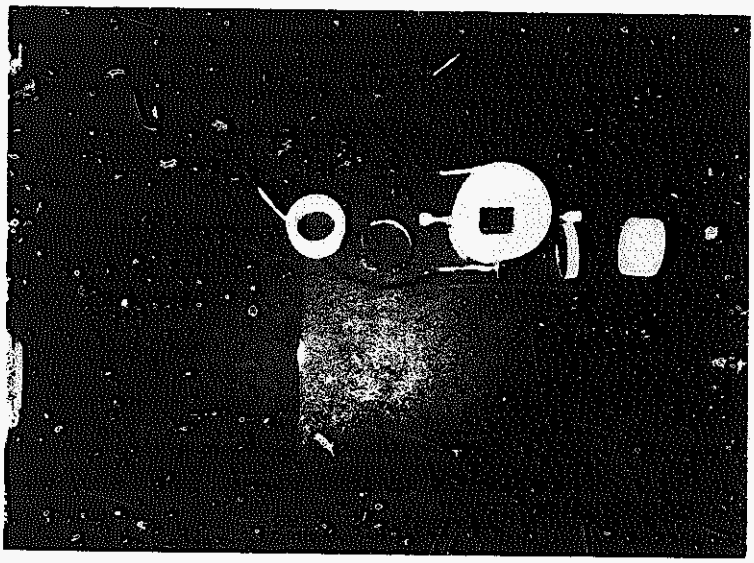

FIGURE 3

(a) Schematic of unshielded and (b) shielded electrode configurations.

(a)

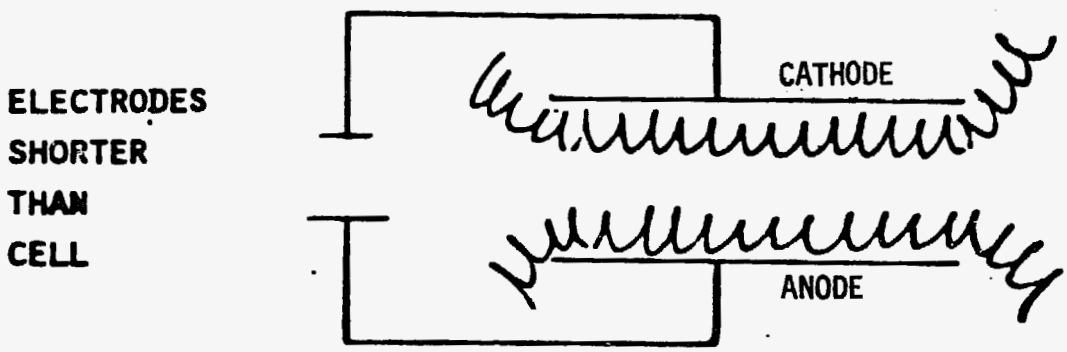

CATHODE: LIGHT LAYER PLUMMING AROUND EDGES AND UPWARD

ANODE: HEAVY LAYER PLUMMING AROUND EDGES AND DOWN-WARD

(b)

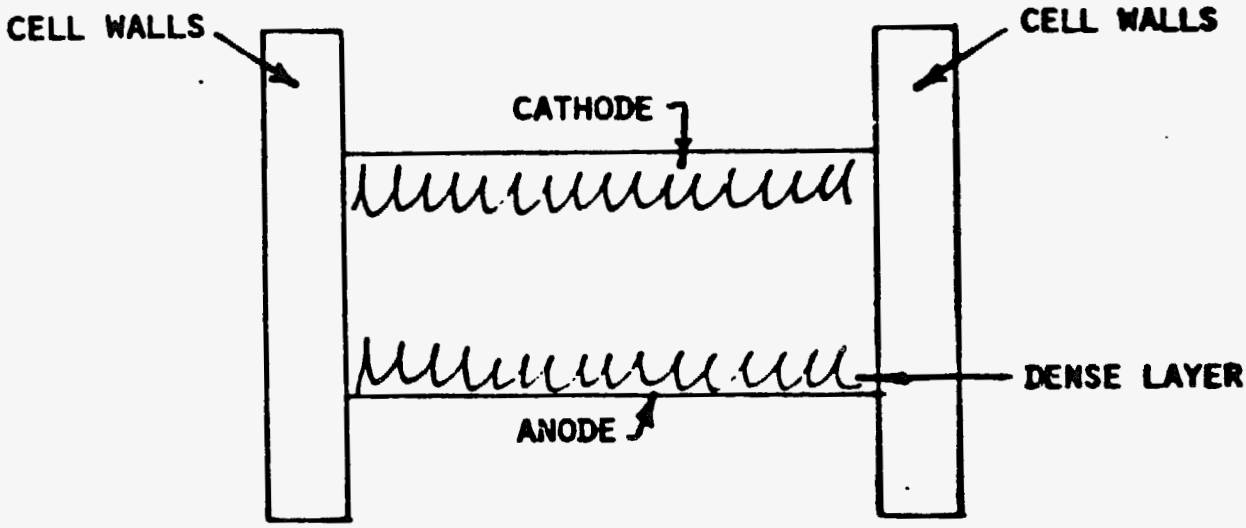

HORIZONTAL CATHODE OVER ANODE WITH ELECTRODE DIMENSIONS THE SAME AS CELL CAVITY. FORCED CONVECTIONLESS SYSTEM FOR 1 g.

the best is an U-V visible rectangular or fluorometric cell with the bottom replaced by an anode of copper or cobalt held by glue. The cell is filled and the cathode held on top with a nylon clamp. The cell must be overfilled so that no bubbles are evident. The cells were used to track the neutral buoyancy particle movement in a shielded configuration.

3.4 Solutions

Copper and cobalt solutions were prepared with spectroscopic grade sulfate salts. The concentrations were determined by titration. The wash water and cobalt solutions for neutral buoyancy work were filtered continuously with .2μm micro filtration until laser detection indicated little or no Brownian motion due to particles larger than .2μm.

3.5 Schlieren/Shadowgraph System

The Schlieren/shadowgraph apparatus utilized was constructed and operated by Dr. Robert Owen of NASA's Space Sciences Laboratory. Owen has described his apparatus in detail.[15-16] Figure 4 depicts a basic schematic of this apparatus that monitors density fluctuations. This system worked on a KC-135 aircraft as well as on the laboratory bench.

3.6 Interferometry

Interferometry replaced Schlieren in order to quantify our data. The interferometer was a Mach-Zehnder type shown schematically in Figure 5. Again this apparatus was constructed from commerically available components by Dr. Robert Owen of NASA's Space Sciences Laboratory. Owen has described this apparatus in detail elsewhere.[17] This apparatus was also successful on a KC-135 aircraft as well as on the laboratory bench. An excellent explanation of the interpretation of interferometry is given by Muller.[18]

Briefly, the data is taken in the form of photographs that record the interferometry fringe pattern. Changes in density appear as fringe shifts that are related to refractive index changes. Thus, a standard curve of refractive index vs concentration enables one to measure concentration change. The initial 35 mm photos are enlarged. The original pictures are utilized with the electrode spacing (1 cm) to set the scale in the enlarged photos. Referring to Figure 6, readings are taken at arbitrary distances from the electrode surface of the fringe shift, Δd. Δd is the distance the center line between two fringes has shifted at that point. The fringe separation in the bulk of the solution is also determined.

FIGURE 4

Schematic of Laser Shadowgraph/Schlieren Apparatus.

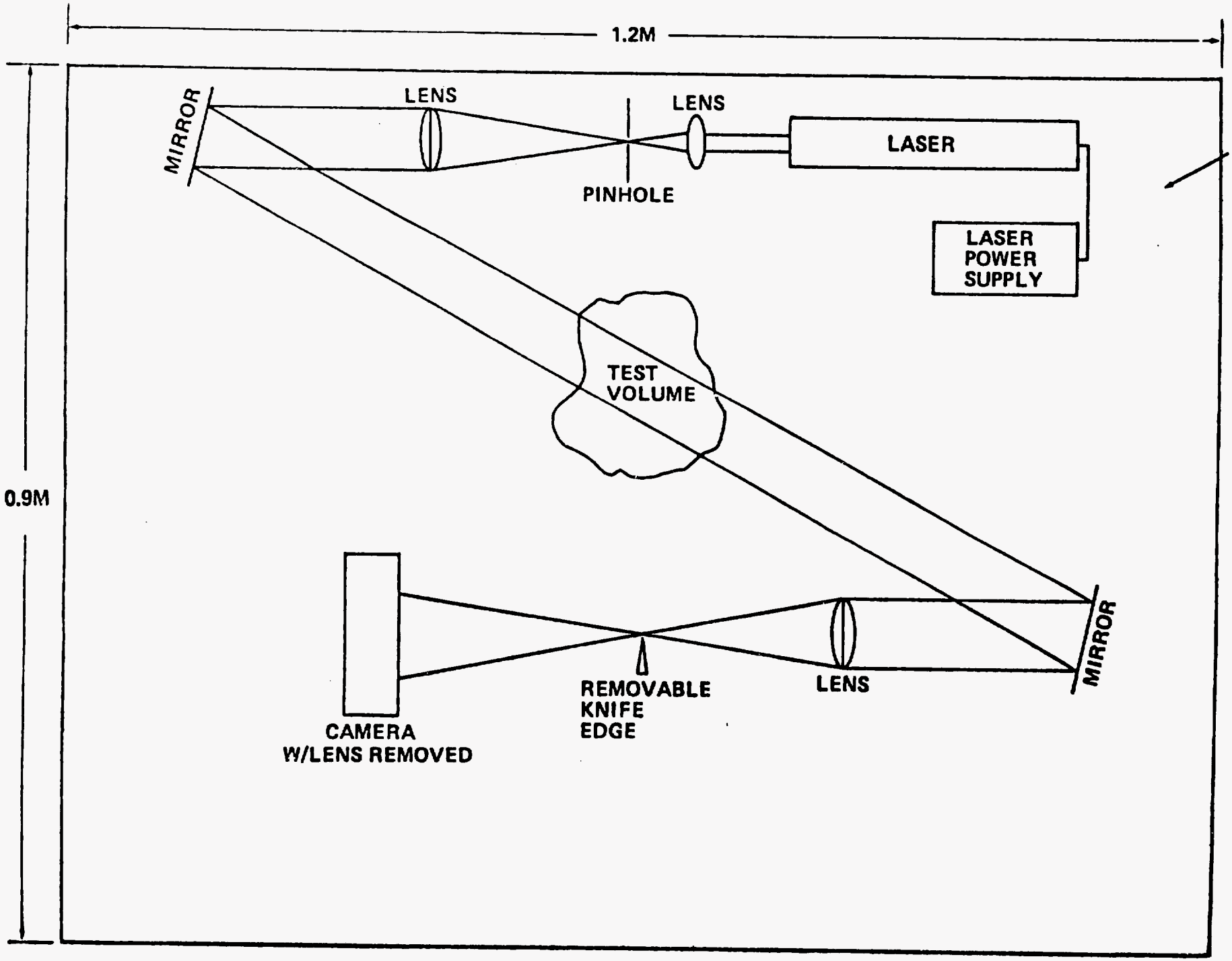

LASER SHADOWGRAPH/SCHLIEREN SYSTEM CONFIGURATION

FIGURE 5

Mach - Zehnder Interferometer

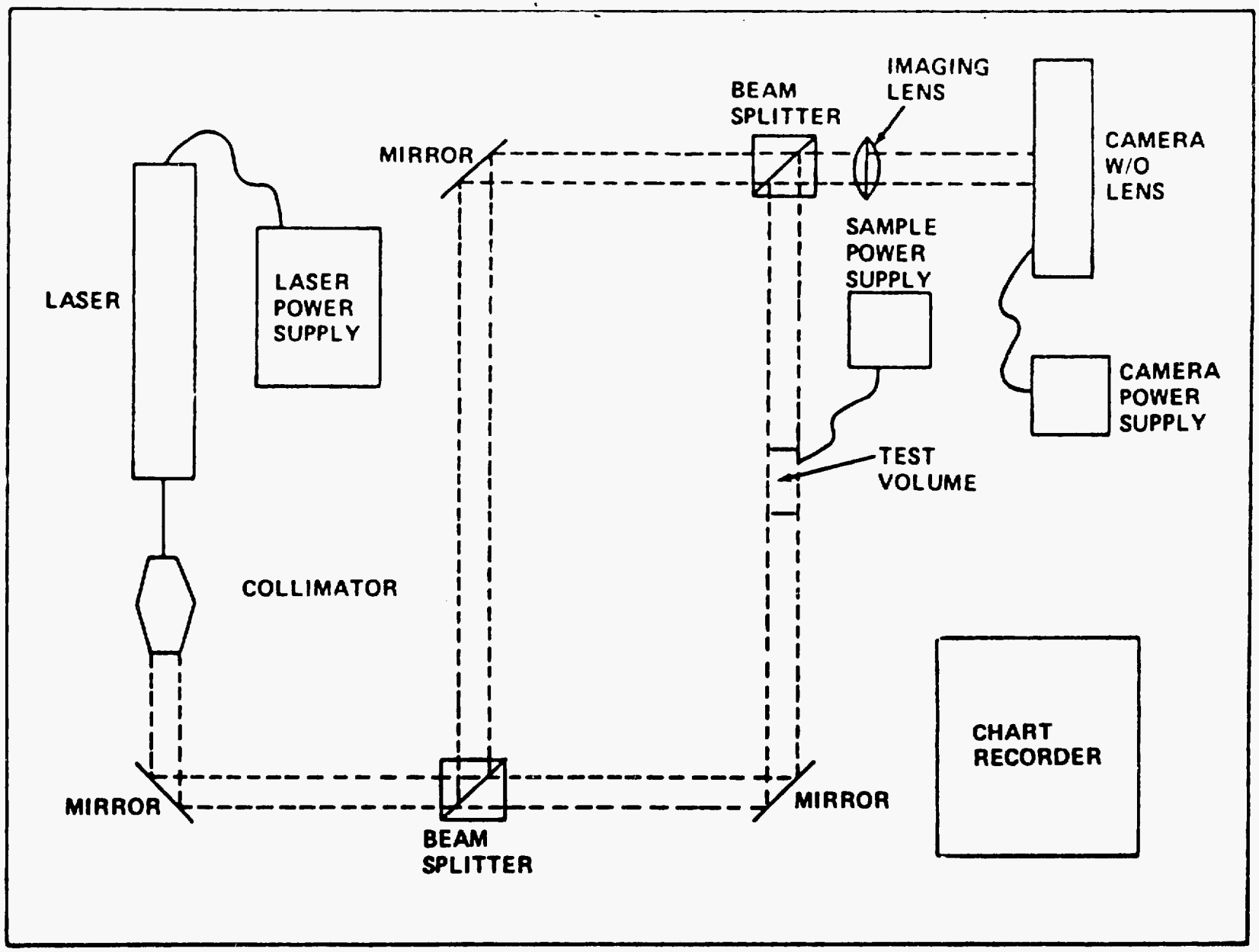

DIAGRAM OF MACH - ZEHNDER INTERFEROMETER

FIGURE 6

Schematic of two fringe curves for determing concentration as a function of distance from the electrode. Δd is the fringe shift at distance 1 from the electrode; d is the fringe separation.

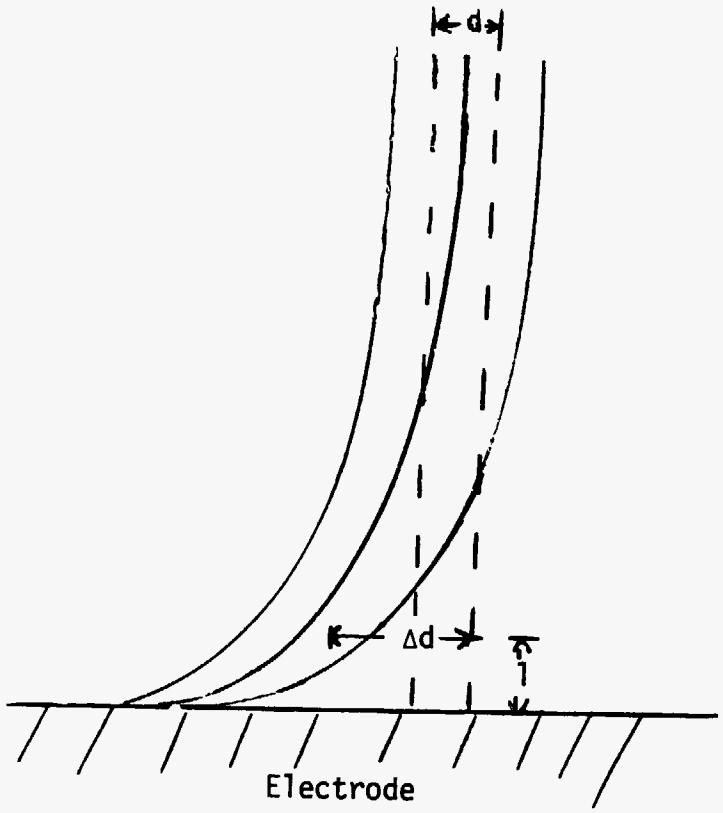

It is designated by d. The change in concentration from the bulk Co denoted by Δc is given by

$$\Delta c = \text{Laser light wave length} \times \frac{\Delta d}{d} \times k \qquad (5)$$

where k is the slope of the curve for refractive index vs concentration of the bulk solution.

Section 4
Results and Discussions

4.1 Unshielded Electrodes and Schlieren Experiments

1 molar $CoSo_4$ was placed in the fluorometric type cells. Typically, current densities ranged from 10-20 mA/cm^2 at voltage less than 1 V. These conditions approximate those used in commerical processes. The low gravity condition was obtained in a NASA KC-135 aircraft by flying porabolic profiles.[15-17] The magnitude of g during the flights was determined by reading a standard aircraft accelerometer. In the low g portion of the path, gravity was usually maintained at $1\text{-}2\times10^{-2}$g.

Figure 7 vividly demonstrates the dramatic effect of gravity reduction upon electrochemical transport. Figure 7A was taken on the bench 12 S after turning on the current. The configuration of anode over cathode was utilized to maximize natural convection between the electrodes. Unstable stratification and advection are evident in the convection currents. Figure 7 B corresponds to the same time, electrode configuration and other experimental conditions as the lab bench study, but at $\sim1\text{-}2\times10^{-2}$g. Convection patterns are not evident, with only the blank pattern typical of the current off condition remaining.

4.2 Shielded Electrodes and Interferometry Experiments

In these experiments we quantify the mass transport by determing concentration changes as a function of distance from the electrode as outlined previously in section 3.6. A typical data graph for a KC-135 10^{-2}g run on copper is depicted in Figure 8. Here we plot concentration change as a function of distance at 10 sec time. This data becomes more meaningful when it is converted to concentration as a function of distance from the electrode. We then become more aware

FIGURE 7

Comparison of convection under different gravity conditions. 7A shows convection density patterns building with horizontal electrodes (anode over cathode) at 1 g. 7B shows lack of convection at low g when all other conditions are identical, including time.

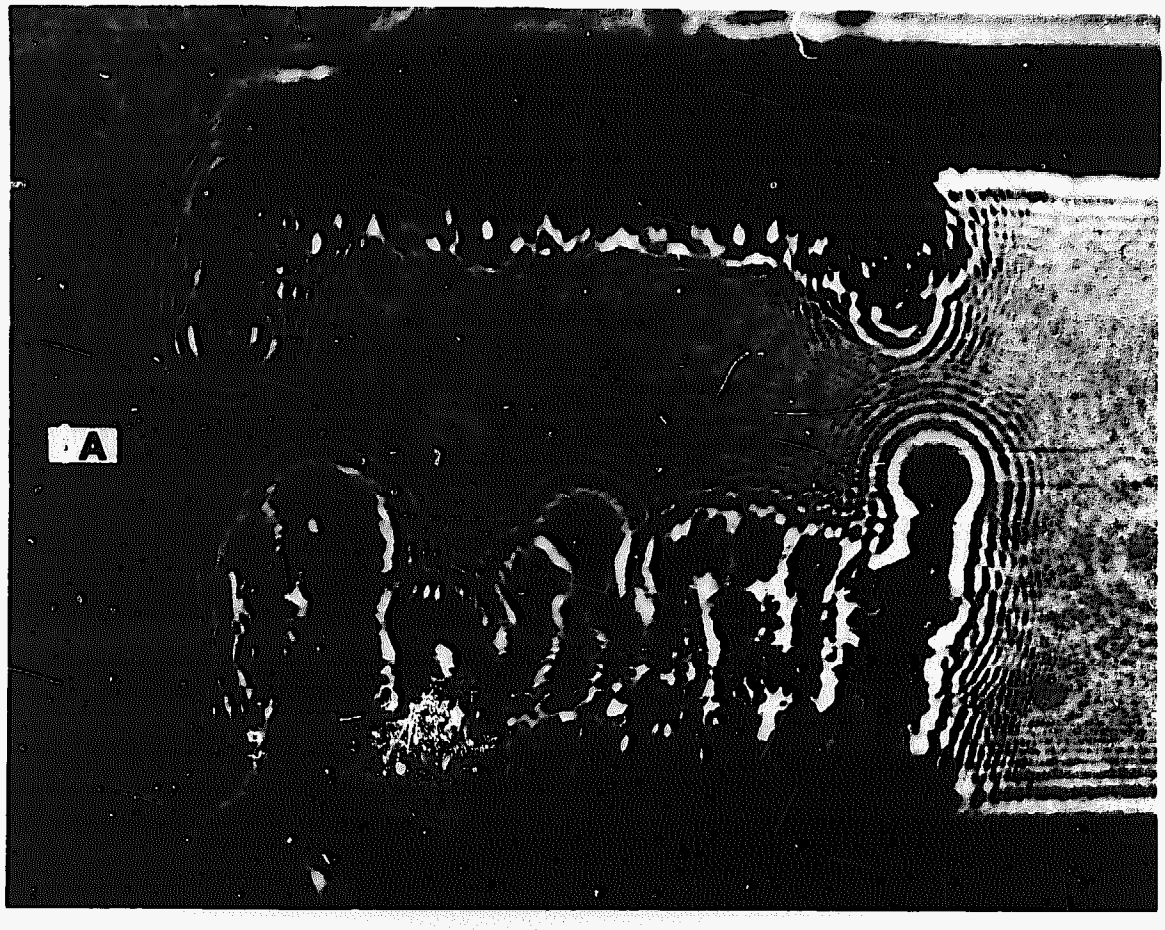

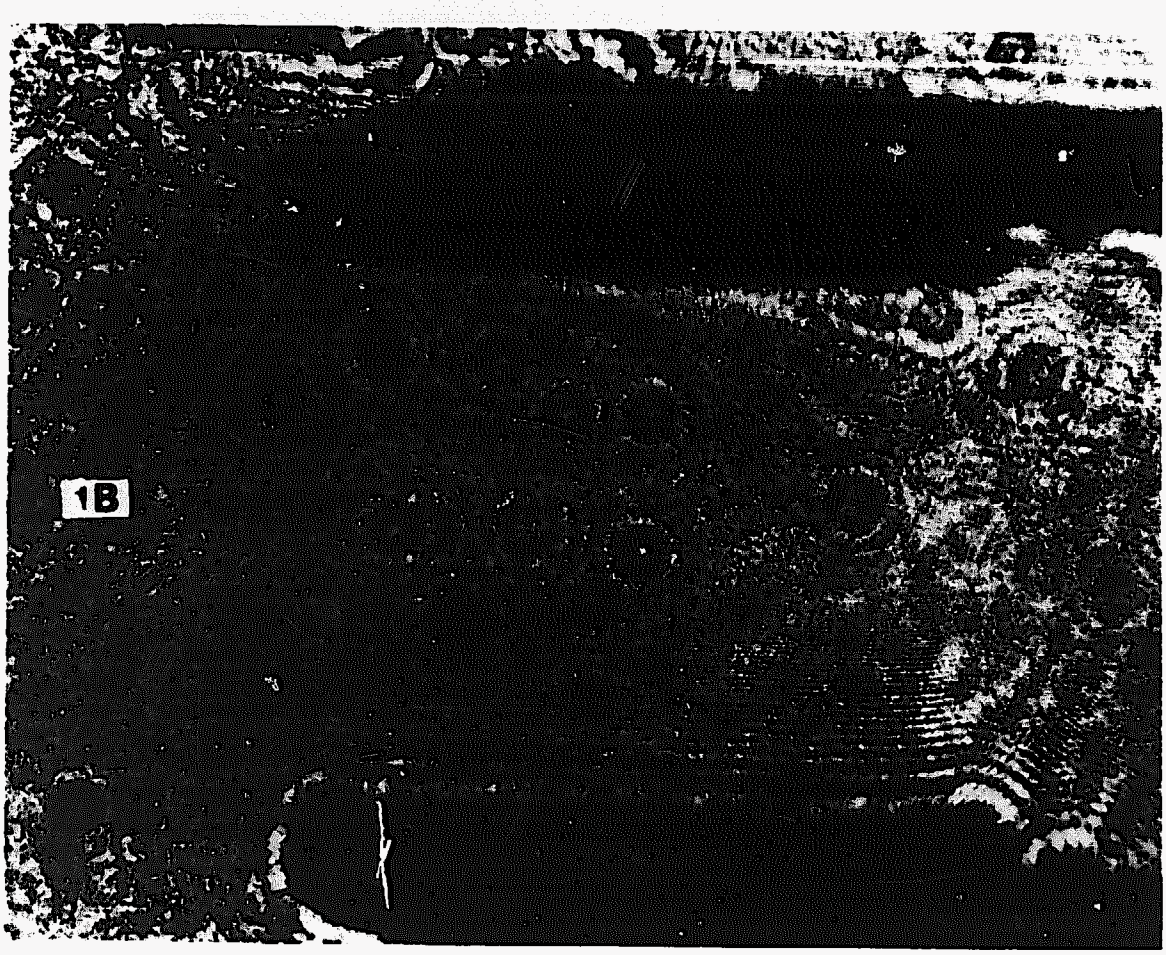

FIGURE 8

ΔC versus distance from electrode .1M Cu at 10 seconds into the run with ~ 10^{-2}g.

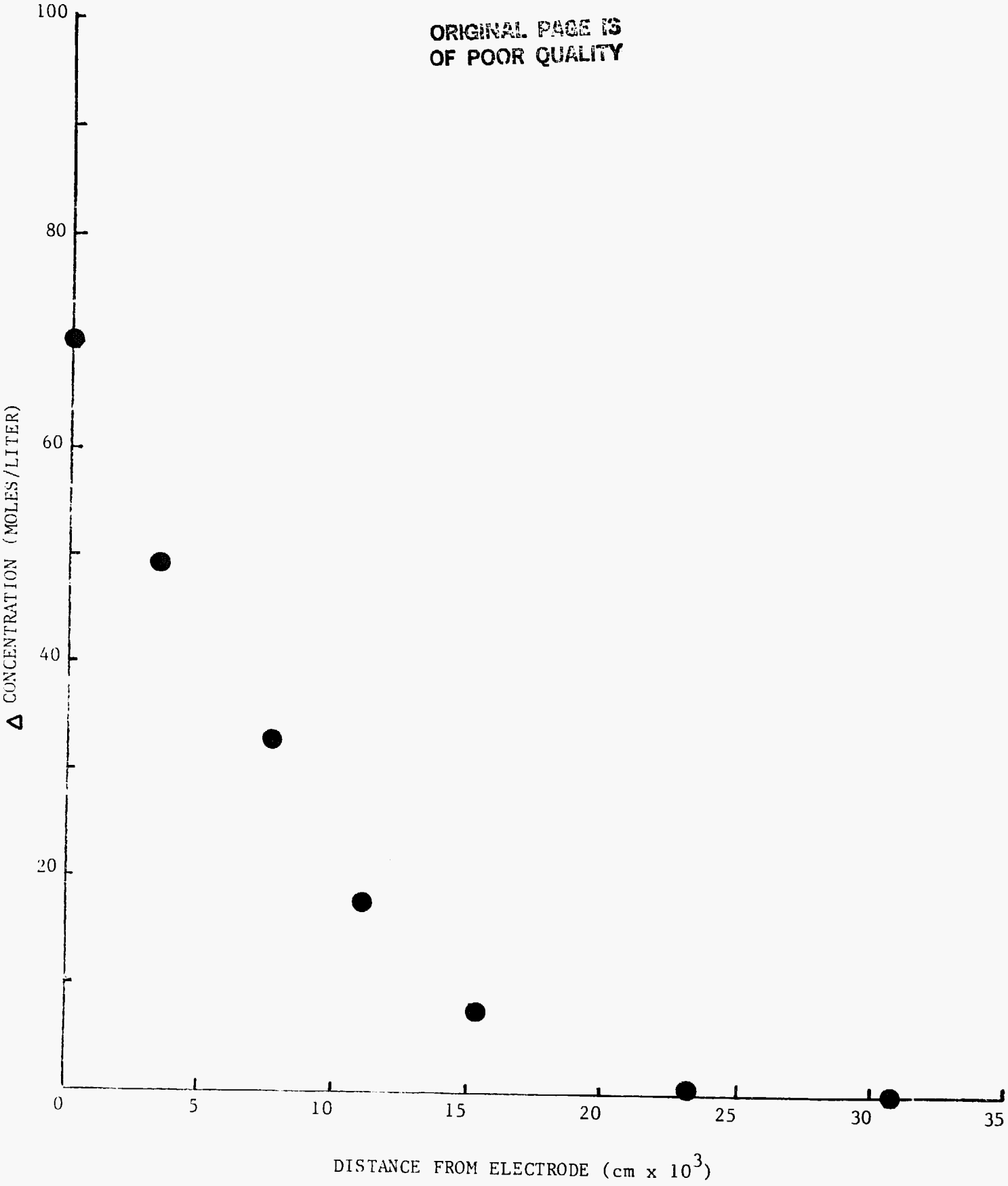

of the parameters bulk concentration Co, extrapolated concentration at the electrode surface Ce, and δ the distance from electrode where the concentration C becomes identical to Co. Figure 9 demonstrates the data in this form. δ_1 is defined as the Nernst diffusion layer thickness and is obtained by extrapolating the linear portion of the curve to the distance from the electrode where C = Co. It can be used to experimentally calculate Ficks first law flux taking the concentration gradient over δ_1 and using literature diffusion coefficients for the particular metal ion:

$$\text{flux} = D\frac{dc}{dy} = D\left(\frac{Co-Ce}{\delta_1}\right). \qquad (6)$$

Comparison of similar data for the same system at identical times on the bench and at $\sim 10^{-2}$ g for 1.0100 M Co are shown in Figure 10A-F at 5, 10, 15 and 20 seconds respectively. The difference between the bench and flight is very evident. The diffusion layer is narrower for the bench relative to the flight study. Equation (6) indicates a greater flux at 1 g than at 10^{-2}g for the cobalt system. Although (Co-Ce) is smaller for the bench, δ_1 is usually smaller by a factor of 2 or so leading to a greater flux at any instant at 1 g. Figures 11A-11D demonstrate the same type of data for .0900 M copper solution. It is not clear from this display whether there is a difference between flight and bench for copper. It should be noted that a factor of $\sim$ 10 in concentration between copper and cobalt exists. The differences we are noting for cobalt could be amplified by this concentration factor. The lower copper concentration was required because of it's strong absorption at 6329 nm, the illumination wavelength of the flight approved laser. If this becomes a major problem, concentration matching could be improved with approval for a different illumination laser.

FIGURE 9

A plot of concentration versus time of the data displayed in Figure 8 for the .0900 M Cu at 10 sec of ~ 10^{-2}g. $\delta_1 = 14.4 \times 10^{-3}$cm is the Nernst diffusion layer thickness and $\delta = 22.2 \times 10^{-3}$ cm is the distance from the electrode at which C = Co.

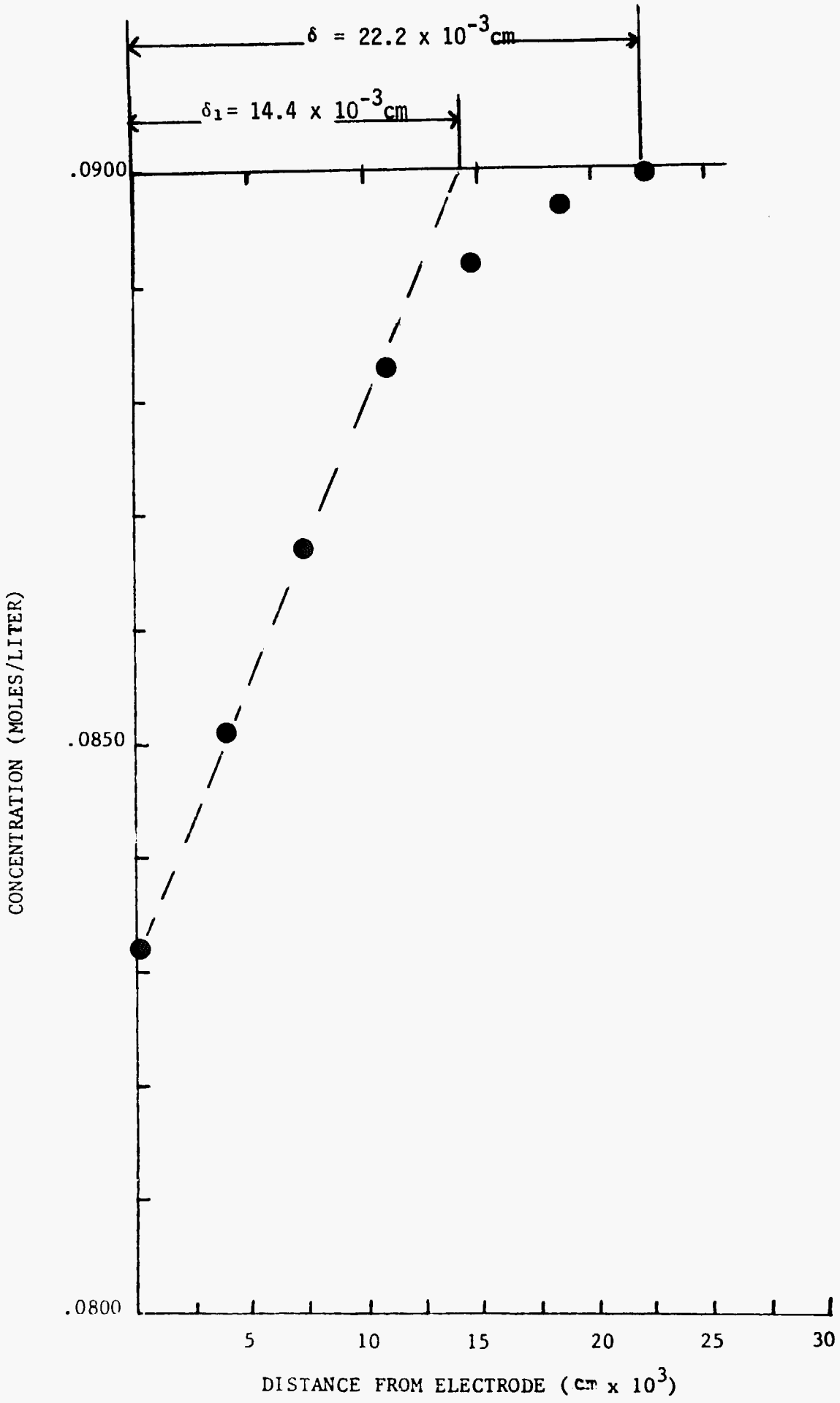

FIGURE 10

Concentration versus distance from electrode for 1.0100 M $CoSO_4$ solution at 10^{-2}g (squares and diamonds) and 1 g (circles). Initial current settings at 14 mA and 15 mA respectively for the flight and 13 mA for the ground. Times into the run are correspondingly 10A - 5 sec, 10B - 10 sec, 10C - 15 sec and 10D - 20 sec. This data was corrected for fringe shifts present at t = 0. Figures 10E and F are identical to 10A and C except no corrections were made for fringe shifts present at t = 0.

A

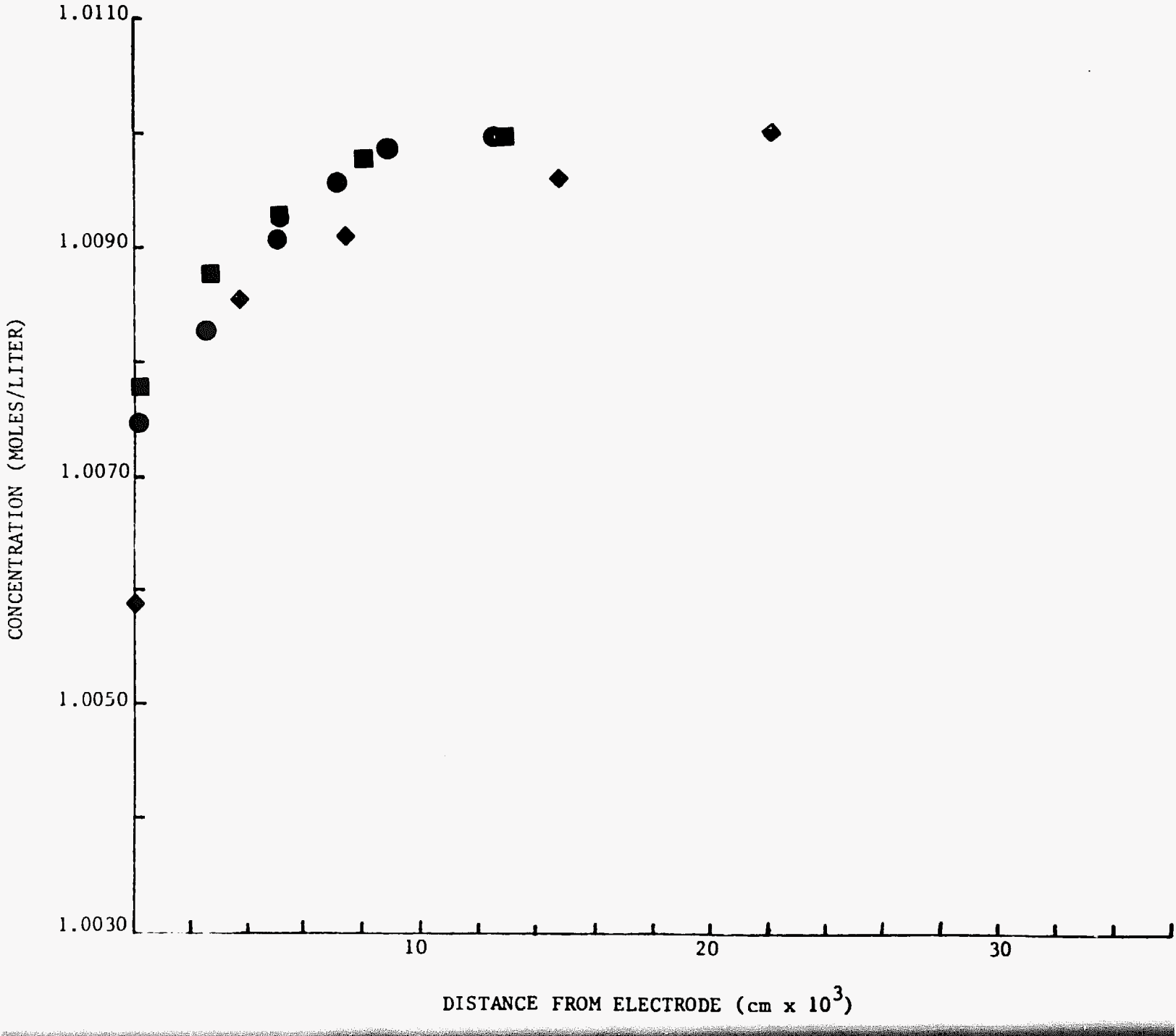

B

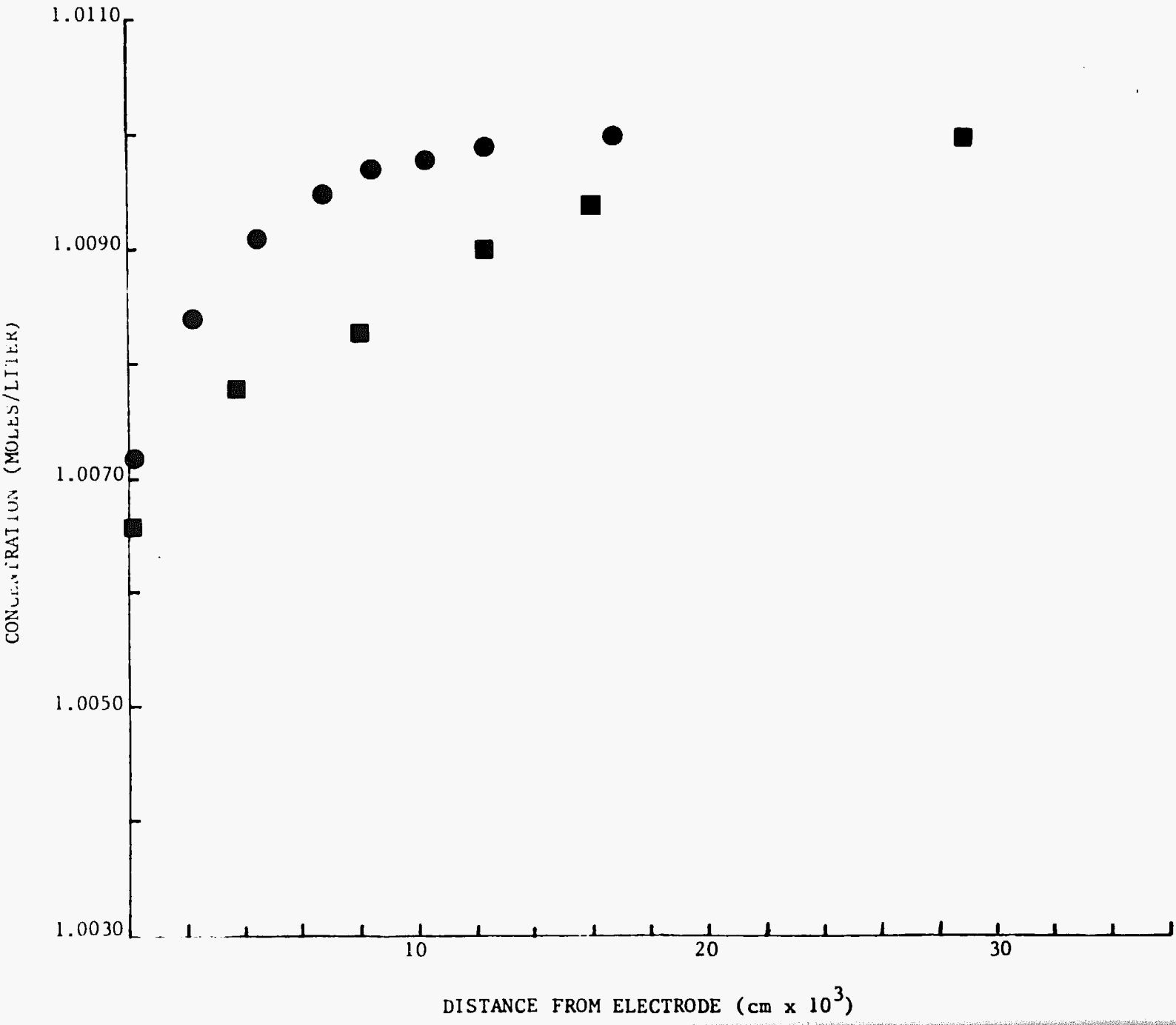

C

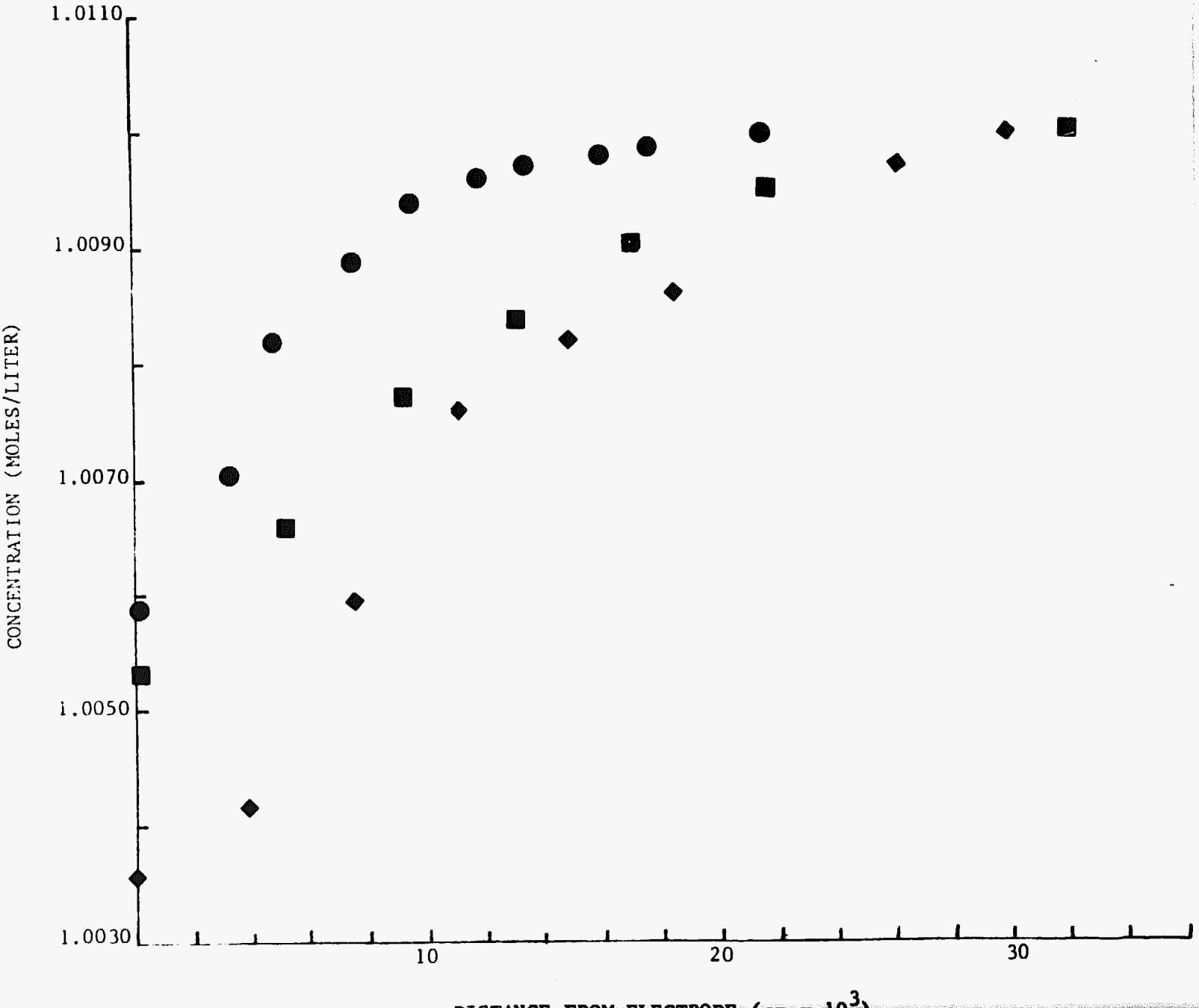

D

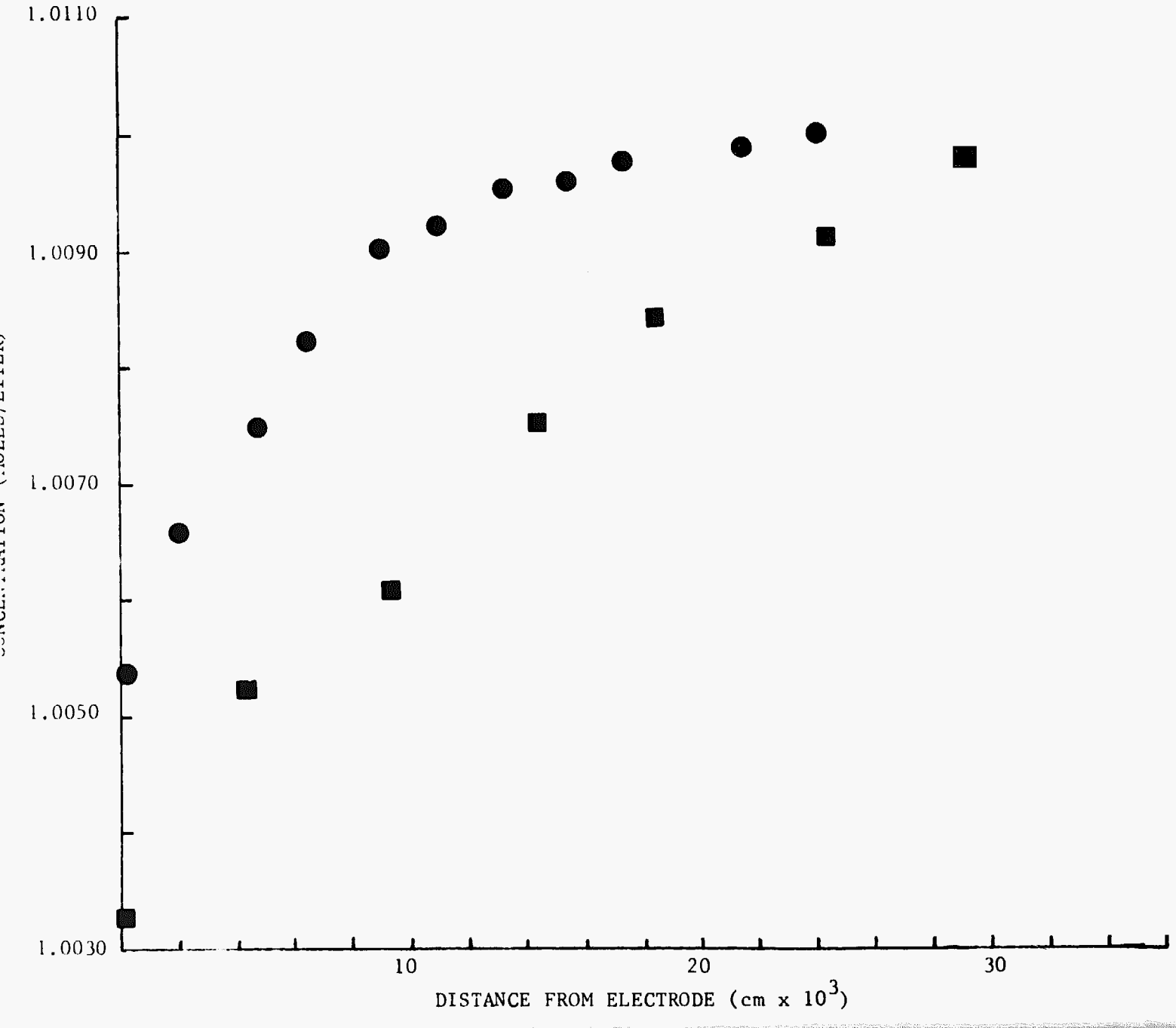

E

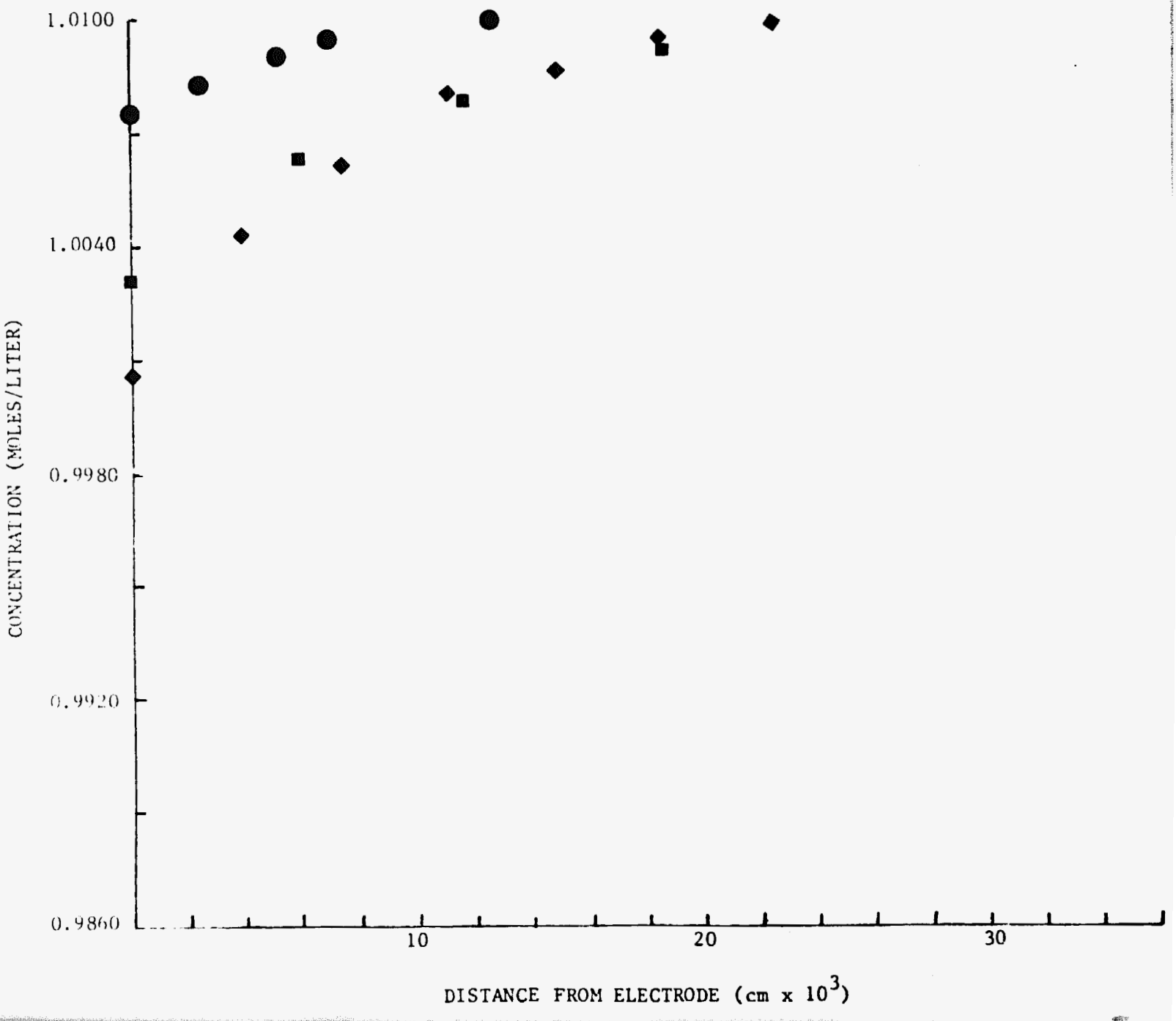

F

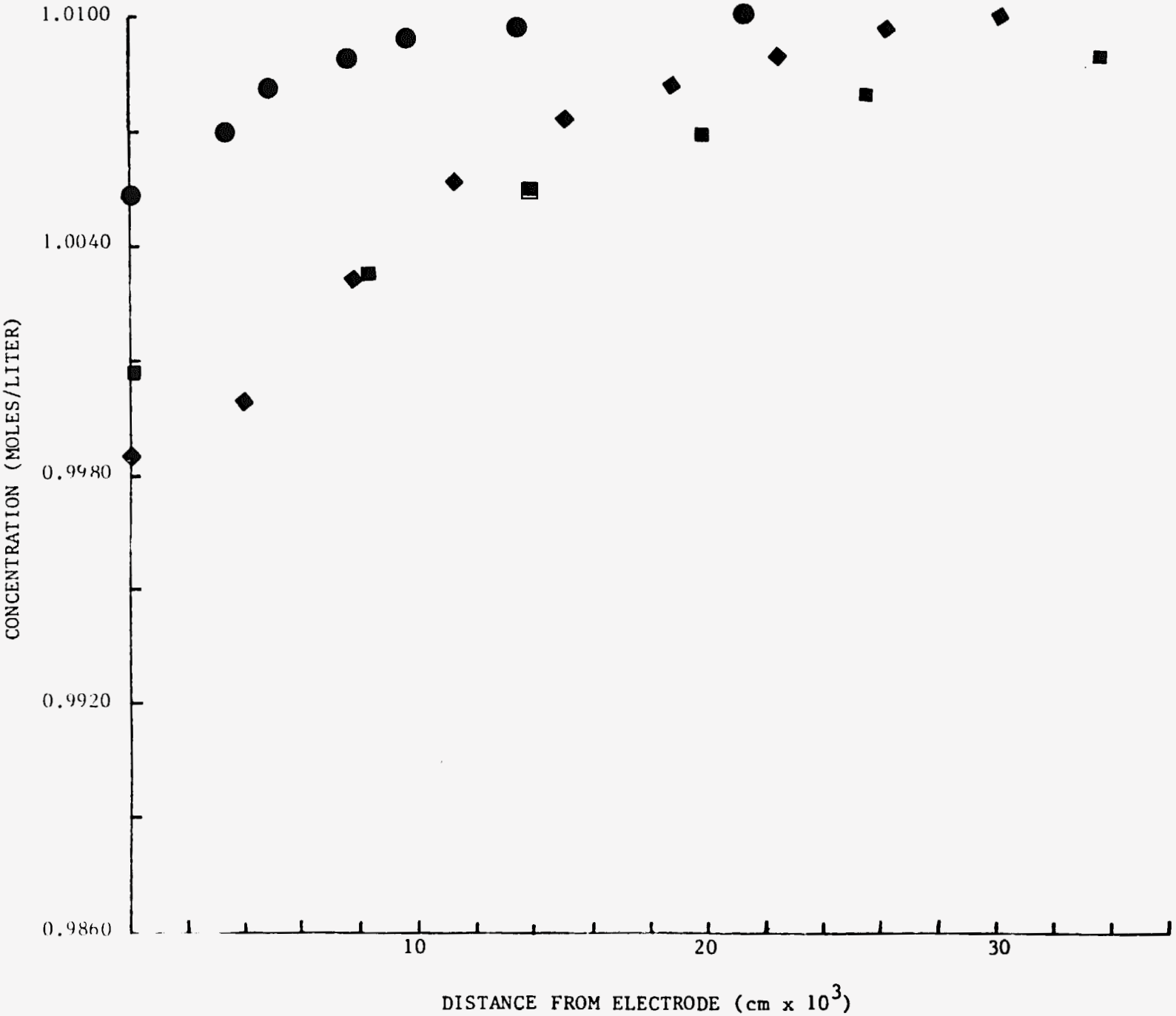

FIGURE 11

Concentration versus distance from electrode for .0900 M $CuSO_4$ at 10^{-2}g (squares) and 1 g (circles). Initial current settings are 14 mA for the flight and 13.5 mA for the ground. Times into the run are correspondingly 11A - 5 seconds, 11B - 10 seconds, 11C - 15 seconds, and 11D - 20 seconds.

A

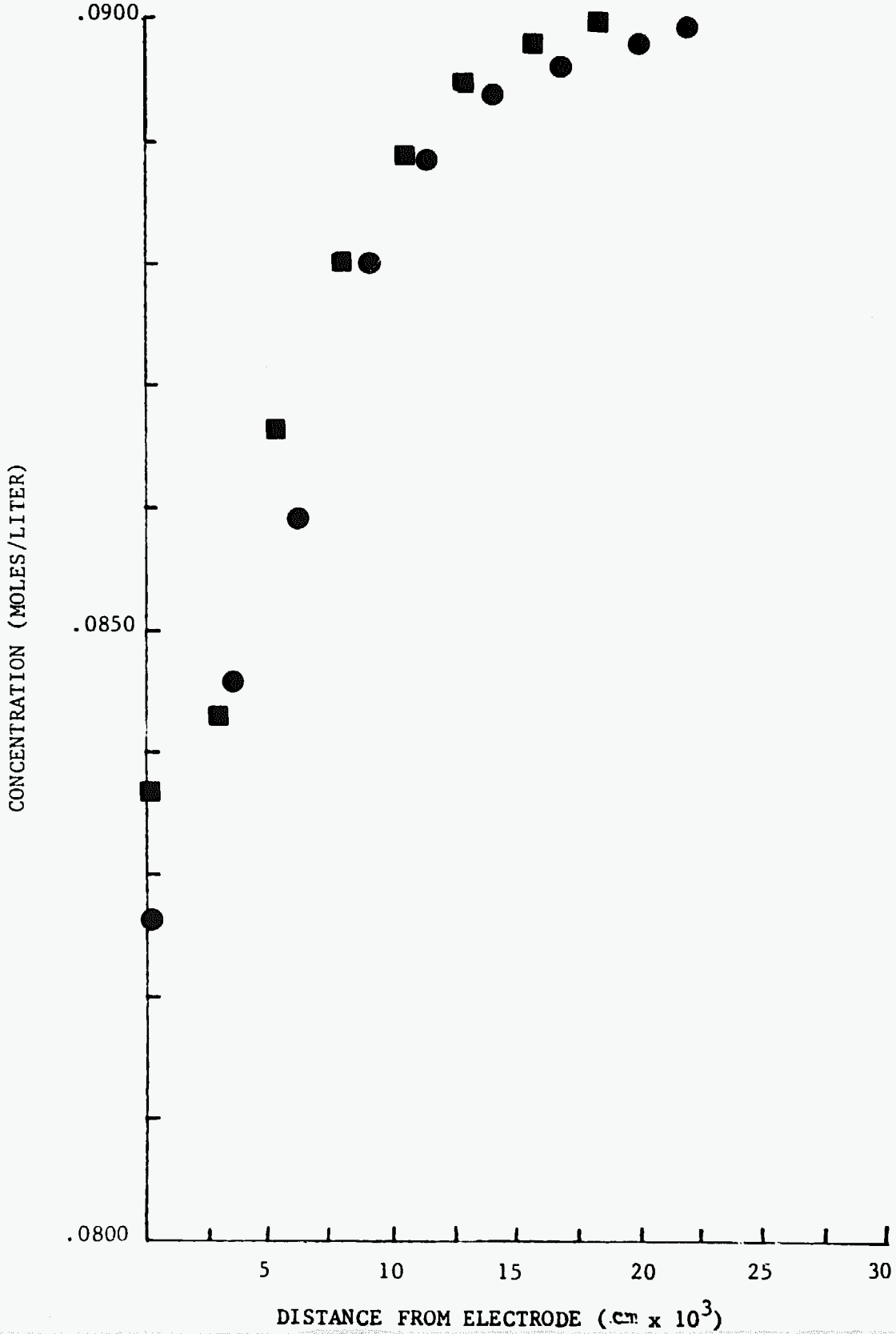

B

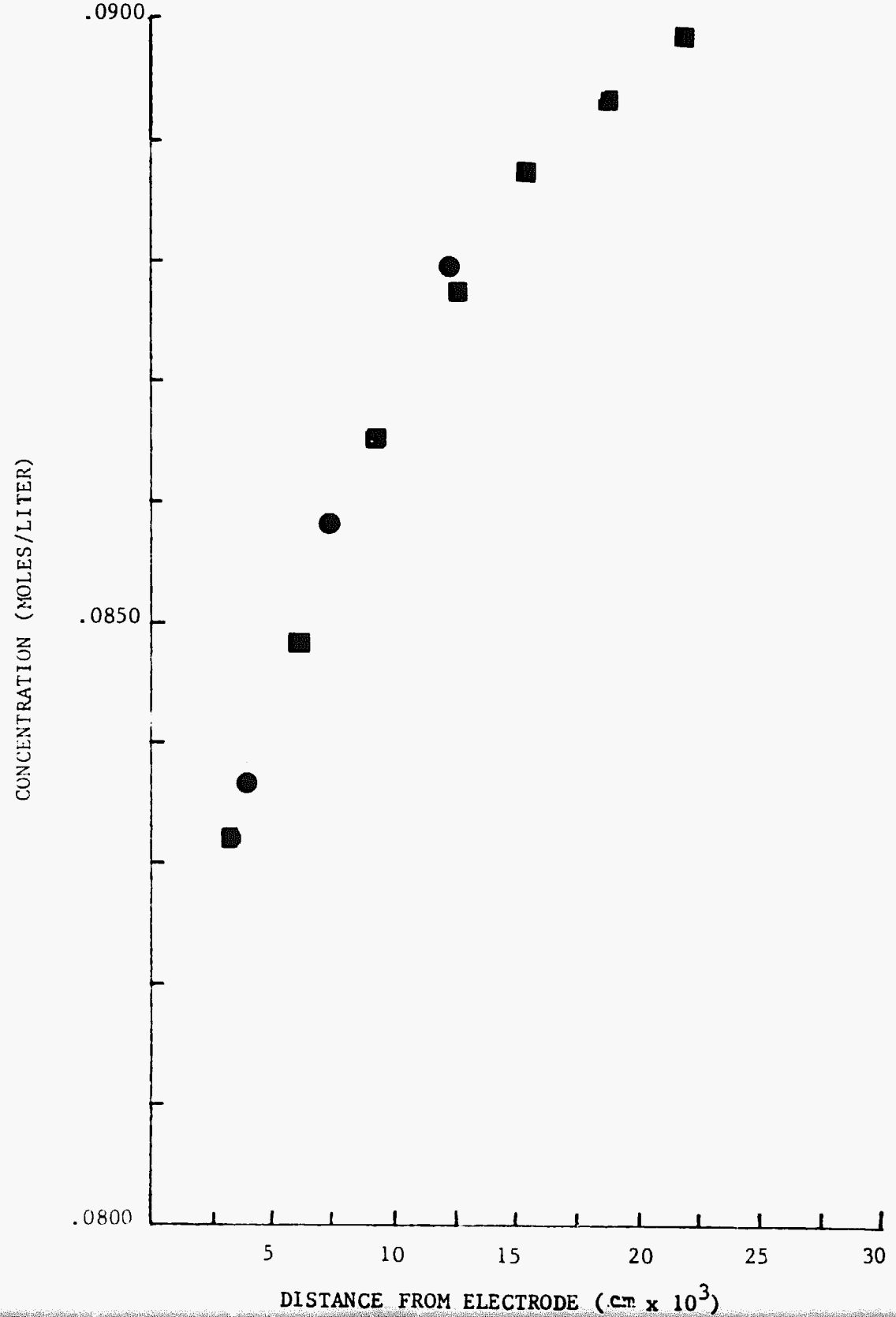

C

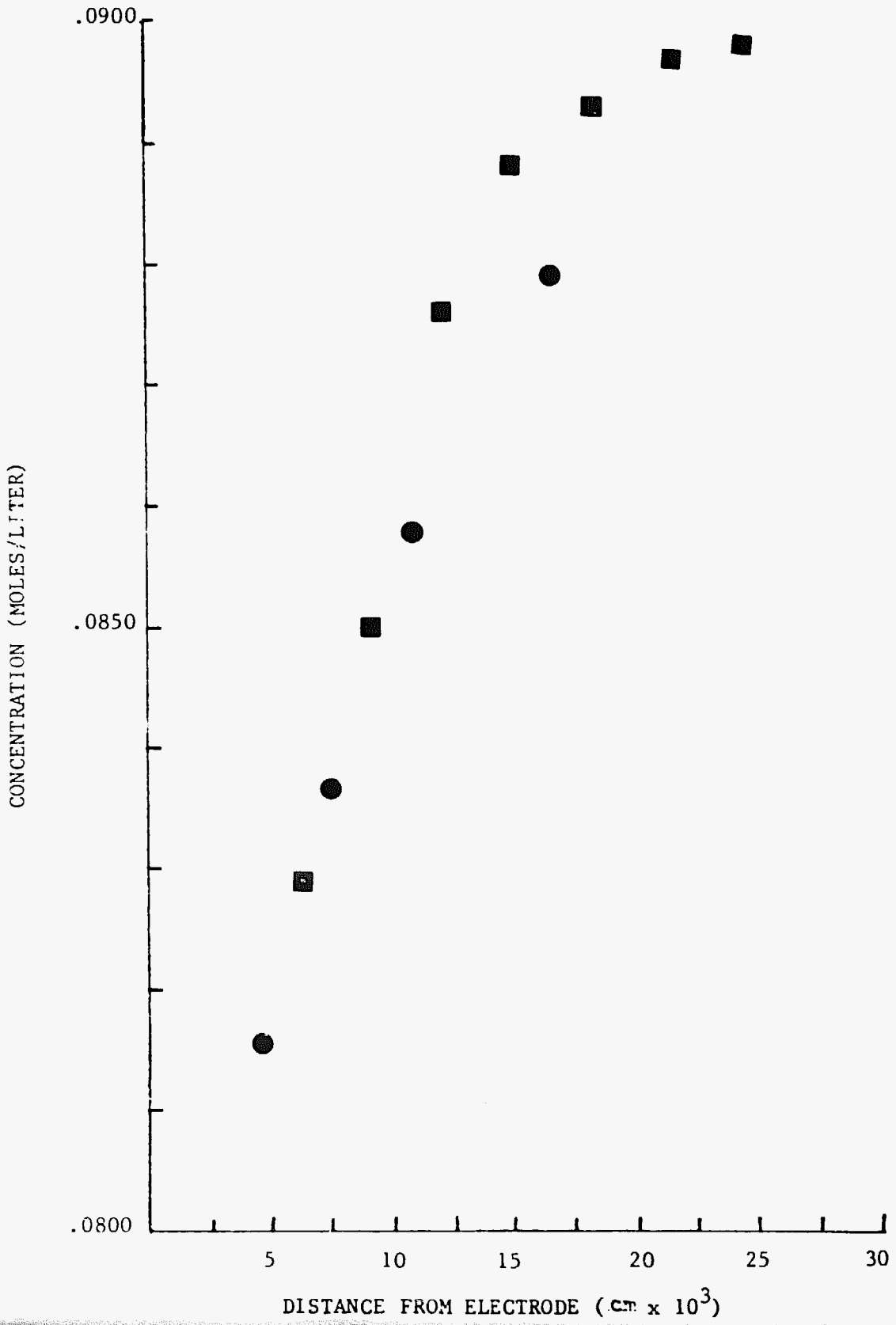

D

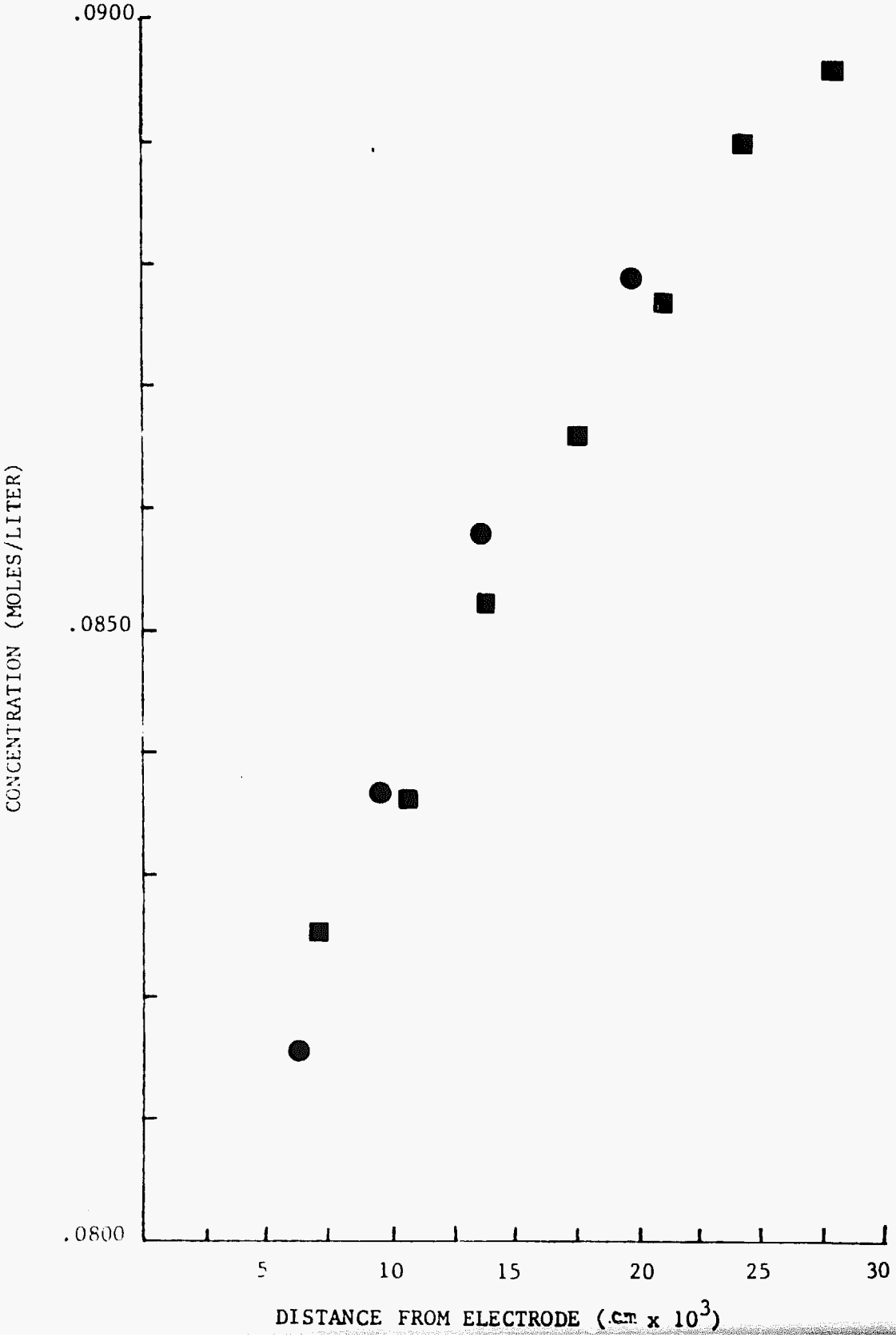

Since there appears to be a difference in diffusion rates for flight and bench we looked for sources of error. One possibility we considered arose in a discussion presented by McLarnon, et al on light deflection errors in interferometry.[19] They argue that erroneous concentrations and diffusion layer thickness determinations due to refraction of rays from the less dense to the more dense bulk solution could arise. This could result in a fringe pattern shift $\Delta\varepsilon$ such that "virtual" fringes appear behind the cathode interface. This shift is given by

$$\Delta\varepsilon = \frac{1}{\lambda o} + \left(\frac{\partial n}{\partial y}\right)^2 + L^3/6n \qquad (8)$$

where λo is the laser wavelength, n is refractive index and L is the cell depth. Y is the axis perpendicular to the electrode surfaces and thus $\frac{\partial n}{\partial y}$ is the refractive index gradients. If one places the collecting lens (subsequent to the cell) far enough away from the cell, all rays (even the most greatly refracted near the electrode surface) should be collected as long as the diffusion layer, δ, does not become too thick. We have not seen any evidence for virtual images to date. We have checked distance between non-working surfaces (stationary bubble) and the electrode interface on interferograms before and after the current was on. No indications of differences were found until the cell had been operational for many minutes. Since our data compares at 20-25 seconds or less, light deflection does not appear to account for our differences.

4.3 Shielded Electrodes and Neutral Buoyancy Experiments

Our first objective was to track the movement of these particles (polystyrene-DVB ($p = 1.06$ g/cm^3). The experiment was designed to determine if there was any significant difference between the motion with the cell operating in a diffusive mode and ordinary Brownian motion. Our first experiments utilized particles with a mean diamter of 11.8 μm which should make them approximately 59 times larger in diamter than any particles remaining after a .2 μm filtration. To date all our photographs indicate no measurable difference in motion. Under these conditions movement was extremely slow of the order 10^{-4}-10^{-5} cm/s. Photographic exposure times of 10 minutes or greater were often required to detect movement (streaks) on the film. We hope with greater magnification that increased speeds closer to the electrode will be detected. They are approximately equal to the speeds in a natural convection driven system and are therefore not negligable.

Our second objective was to look at the parameters that affect the codeposits. In our first attempts we obtained very inhomogenous distributions (clumps) of neutrals in the deposited cobalt. We attribute this to undulations in the cathode. A highly polished surface will be required to have random attachment of the neutrals for subsequent entrapment in the depositing metal matrix. We are confident 600-800 grit preparation will eliminate this initial difficulty enabling concentration on parameters such as current, PH, cermet concentration and temperature.

Section 5
Summary and Conclusions

The primary objective of this work was to study the effects of gravity driven convection on the electrodeposition processes and products. This goal has been achieved. In addition, the NASA contingent of the cooperative effort developed and tested an interferometer for flight studies at 10^{-2}g, and preliminary studies using this detection system indicate there is a difference in the magnitude of diffusion controlled flow on the bench relative to flight.

Our work with Schlieren on the cobalt system demonstrated pictorially the effect of gravity upon natural convection. Although, one may conclude this was an "obvious result", to our knowledge it had never been demonstrated especially in a manner easily interpreted by laymen. After development of a flyable interferometer quantitative studies on diffusion controlled flow produced in shielded electrode cells indicated that a cobalt system has greater diffusive flow at 1 g than at 10^{-2}g. Data from similar experiments on a copper system were inconclusive.

A shielded electrode cobalt cell was developed for neutral buoyancy experiments. Tracking the movement of the particles under diffusive conditions showed no detectable difference relative to ordinary thermal or Brownian motion. Unless the differences were significant, an order of magnitude or more, it probably would not be within the resolution of our experiment which involved photographing laser light reflected from particle surfaces. Characterizing the codeposits produced in these cells as a function of various parameters was started. Clumping of the polystyrene codeposits on the cathode impeded our progress. We attribute the difficulty to cathode surface roughness and worked out a preparative technique which produces a uniform surface observed at 70X magnification. Hopefully this will result in more homogeneous codeposition. Regardless, the cell and neutral buoyancy

particles appear to work and should lead to important scientific data. It also will be most interesting to determine if deposits produced in a shielded electrode system offer greater corrosive resistance than one produced during natural or forced convection conditions.[20]

Section 6

REFERENCES

1. Ralph N. Adams, Electrochemistry At Solid Surfaces, Marcel Dekker, Inc. New York, (1969), Chapter 3. "Mass Transfer To Stationary Electrodes In Quiet Solutions".

2. R. N. O'Brien, W. F. Yakymyshyn, and J. Leja, "Interferometric Study of Zn/$ZnSO_4$/Zn System I", J. Electrochem. Soc., 110, 820 (1963).

3. R. N. O'Brien, "Concentration Gradients at Horizontal Electrodes", J. Electrochem. Soc., 113, 389 (1966).

4. R. N. O'Brien, C. A. Rosenfield, K. Kinoshita, W. F. Yakymyshyn, and J. Leva, "The Dependence of Concentration Gradient on Current Density at Working Electrodes", Can. J. Chem., 43, 3304 (1965).

5. R. N. O'Brien, J. Leja and E. A. Beer, "Interferometric Study of the Zn/$ZnSO_4$Zn System II", J. Electrochem Soc., 121, 370 (1974).

6. R. N. O'Brien and Henry K. Kolny, "An Interferometric Study of a Convectionless Steady State of Concentration Polarization", Can. J. Chem., 56, 591 (1978).

7. R. B. Owen, "Proceedings of OSA/SPID Huntsville Electro-Optical Technical Symposium, Huntsville, AL. September 19 - October 3, 1980.

8. L. A. Vasilev, Schieren Methods, Keter Publishers Ltd., London (1971).

9. E. A. Brandes, and D. Goldthrope, "Electrodeposition of Cermets", Metallurgia, 195 (Nov. 1967).

10. T. W. Tomaszewki, L. C. Tomasgewaki and H. Brown, "Codeposition of Finely Dispersed Particles with Metals", Plating, 1234 (Nov. 1969).

11. E. C. Kedward, C. A. Addison and A. A. B. Tennett, "The Development of a Wear Resistant Electrodeposited Composite Coating for Use on Aero Engines" Trans. Inst. Metal Fin. 54, 8 (1976).

12. D. W. Snaith and P. D. Groves,"A Study of the Mechanisms of Cermet Electrodeposition", Trans. Inst. Met. Fin., 50, 95 (1972).

13. P. W. Atkins, Physical Chemistry, 2nd Edition, W. H. Freeman and Company, San Francisco, (1982) page 846.

14. N. Guglielmi, "Kinetics of the Deposition of Inert Particles from Electrolytic Baths", J. Electrochem. Soc., 119, 1009 (1972).

15. Robert B. Owen, "Optical Measurements and Tests Performed in a Low-Gravity Environment", SPIE, Vol. 255, P74 (1980)

REFERENCES (continued)

16. Robert B. Owen, "Laser Shadowgraph and Schlieren Studies of Gravity-Related Flow During Solidification", Optics and Lasers in Engineering, Vol. 2, page 129 (1981)

17. Robert B. Owen, "Interferometry and Holography in a Low Gravity Environment", App. Opt. Vol. 21, No. 8, Page 1349 (1982)

18. R. H. Muller, in Advances in Electrochemistry and Electrochemical Engineering, edited by P. Delahay and C. W. Tobias, Vol. 9, pp. 281-368, John Wiley and Sons, New York 1973.

19. F. R. Meharnon, R. H. Muller, and C. W. Tobias, "Light-Deflection Errors in the Interferometry of Electrochemical Mass Transfer Boundary Layers", J. Electrochem. Soc. 122, 59 (1975)

20. J. Ehrhardt, "Versuche Zur Elektrolytischen Metallabscheidung unter Schwerelosigkeit", Galvanotechnik, D 7968, Saulgan 72, 13 (1981)